Available online at www.sciencedirect.com
ScienceDirect
Journal of Power Sources 175 (2008) 909–913
JOURNAL OF POWER SOURCES
www.elsevier.com/locate/jpowsour

Short communication

Fiber-based flexible thermoelectric power generator

A. Yadav [a], K.P. Pipe [a], M. Shtein [b,*]

[a] *Department of Mechanical Engineering, 2350 Hayward Street, University of Michigan, Ann Arbor, MI 48109, United States*
[b] *Department of Materials Science & Engineering, 2300 Hayward Street, University of Michigan, Ann Arbor, MI 48109, United States*

Received 6 August 2007; accepted 24 September 2007
Available online 6 October 2007

Abstract

Flexible thermoelectric power generators fabricated by evaporating thin films on flexible fiber substrates are demonstrated to be feasible candidates for waste heat recovery. An open circuit voltage of 19.6 μV K per thermocouple junction is measured for Ni–Ag thin films, and a maximum power of 2 nW for 7 couples at $\Delta T = 6.6$ K is measured. Heat transfer analysis is used to project performance for several other material systems, with a predicted power output of 1 μW per couple for Bi_2Te_3/Sb_2Te_3-based fiber coatings with a hot junction temperature of 100 °C. Considering the performance of woven thermoelectric cloths or fiber composites, relevant properties and dimensions of individual thermoelectric fibers are optimized.

Keywords: Flexible power generator; Thin film thermoelectrics; Convectively cooled thermoelectrics; Waste heat recovery

1. Introduction

Thermoelectric (TE) power generators can be used in many cases to improve the efficiencies of mechanical and electrical devices by converting waste heat energy to electrical power. Such generators are typically fabricated from [bulk] semiconductors such as Bi_2Te_3 and SiGe, making them rigid and unsuitable for covering large areas. In order to improve thermal contact to heat sources of arbitrary geometry, it is desirable to produce thermoelectric generators which can conform easily to a surface. However, devices based on flexible thermoelectric materials such as organic semiconductors have proven impractical to date due to low intrinsic electrical carrier mobility [1]. Another approach involves embedding discrete miniature TE chips in a flexible matrix, but suffers weight penalties associated with bulk materials and potentially entails complex and expensive fabrication.

A more desirable configuration is a thin film-based, flexible and lightweight thermoelectric device which may be fabricated in a cost-effective reel-to-reel fashion. Energy conversion using flexible devices is a concept which is finding broad application in many energy-harvesting devices. These include photovoltaic cells [2] and organic light emitting diodes (OLED) [3] fabricated by depositing thin films on flexible substrates and flexible piezoelectric membranes or fibers [4,5]. In addition, miniaturization of energy conversion devices is also attractive for powering low power electronics using readily available energy sources such as human body heat [6], heel strikes in walking [6], etc.

Previous work in flexible thermoelectric power generators has involved fabrication of multiple thermocouple junctions on flexible planar substrates. Itoigawa et al. [7] used a wavy polyimide sheet with junctions at the top and bottom of the sheet to build a flexible thermopile. Sato and Takeda [8] used a combination of copper and polyimide sheets as a flexible substrate to create an inplane temperature gradient from a crossplane heat flux. Both of these techniques require photolithography and precision machining, and their flexibility is limited by the thickness of the substrate. Here we propose and demonstrate a flexible thermoelectric generator based on thin film thermoelectric junctions on flexible fibers. These fibers can be woven into energy-harvesting fabrics or can be interwoven with structural fibers such as carbon fibers to create an energy-harvesting composite. We deposit thin films using thermal evaporation, a technique which can be readily scaled up in a high-throughput

* Corresponding author. Tel.: +1 734 764 4312; fax: +1 734 763 4788.
E-mail address: mshtein@umich.edu (M. Shtein).

0378-7753/$ – see front matter © 2007 Published by Elsevier B.V.
doi:10.1016/j.jpowsour.2007.09.096

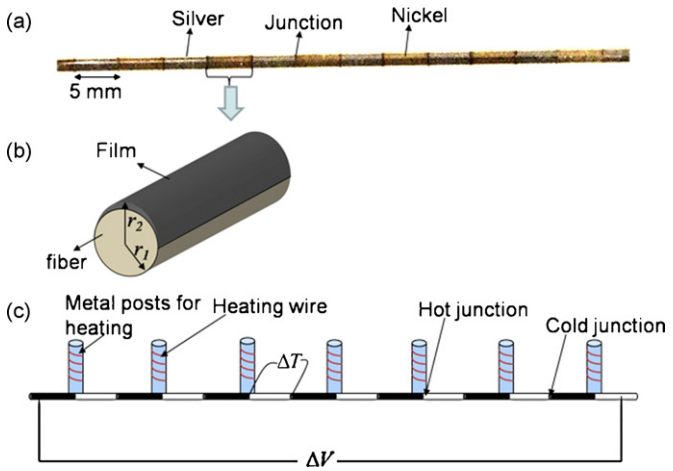

Fig. 1. (a) Picture of striped thin film thermoelectric fiber made with thermal evaporation of nickel and silver. (b) Illustration of fiber with thin film deposited on one side. (c) Schematic of experimental setup for applying a temperature gradient and measuring the induced open circuit voltage.

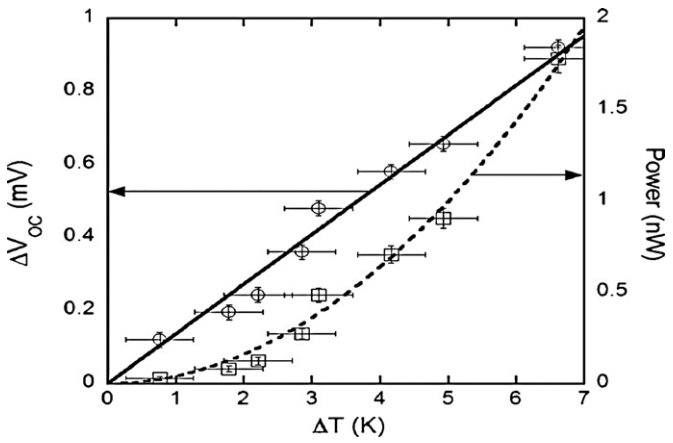

Fig. 2. Net thermal voltage and maximum power output as a function of temperature applied for 7 couples.

reel-to-reel fashion for the fabrication of devices such as thin-film solar cells and organic LEDs. To prevent abrasion of the thermoelectric coating or electrical shorting, the fibers can be easily coated with a light-weight plastic barrier film, either by solution coating, or by chemical vapor deposition [9]. Weaving techniques used in common textiles or those specifically developed for electronic textiles [10] can be used to establish robust parallel and series electrical interconnects.

2. Fabrication method and testing procedure

Thin-film metallic thermocouples are a convenient basis for the proof-of-concept demonstration of thermoelectric fibers. Adjacent stripes of nickel and silver are deposited on one side of a silica fiber of diameter 710 μm by thermal evaporation under a vacuum of 5×10^{-7} Torr, as shown in Fig. 1a and b. First a silver layer of thickness 120 nm is deposited through a mask; the mask is then moved to cover the deposited silver, and a nickel layer of thickness 120 nm is deposited. The junctions are formed by a 0.5 mm overlap between the two metals.

To test the thermoelectric properties of the fiber, we heat alternate junctions, resulting in a temperature gradient that mimics the heating profile of the fiber inside a woven pattern which has a temperature gradient normal to the surface. As shown in Fig. 1c, we use electrically insulated posts with heating wire wrapped around them as heat sources, bringing alternate fiber junctions in contact with them. The unheated junctions are exposed to ambient (22 °C) and lose heat due to convection. Temperature differences between neighboring junctions are measured using microthermocouples. Open circuit voltage versus temperature is measured, as well as the induced voltage across a matched load resistor.

3. Results and discussion

The resistance of the thermoelectric fiber is measured to be 123 Ω, which includes the contact resistance between gold wires and the ends of the TE fiber. This gives a total resistivity of 470 nΩ m for Ni–Ag, which is higher than literature values of 190 nΩ m [11] for vacuum evaporated nickel and 20 nΩ m [12] for vacuum evaporated silver. The larger resistivity is attributed to junction and contact resistivity, as well as film quality.

In Fig. 2 the open circuit voltage developed as a function of temperature difference (ΔT) between the junctions and the maximum power output is plotted. The net open circuit voltage is sum of the thermoelectric voltage developed over all the junctions. A linear fit to the experimental data yields a Seebeck coefficient of 19.6 ± 0.6 μV K, which agrees well with the bulk theoretical value for the Ni–Ag junction of 19.2 μV K [13]. The measured Seebeck coefficient shows no dependence on film thickness or substrate geometry. The maximum generated power is measured by placing a load resistor with resistance matched to that of the fiber and is given by:

$$P_{\max} = \frac{n^2 S^2 \Delta T^2}{4R_f} \tag{1}$$

where $P_{\max}$ is the maximum power output, S is the net Seebeck coefficient of each junction, n is the number of thermocouples, and R_f is the total electrical resistance of the fiber which can be written as (idealizing for the case of no added junction resistance):

$$R_f = \left(\frac{\rho_e}{A_e} + \frac{\rho_p}{A_p}\right) nl \tag{2}$$

where ρ_e and ρ_p are the electrical resistivity of n and p segments and A_e and A_p are respective cross-sectional areas. The maximum power increases as the square of the temperature difference applied, which is seen in the experimental data in Fig. 2. The internal resistance of the fiber and the combined Seebeck coefficient of the junction also affect the power output. Fig. 3 plots the voltage and power versus the current produced by a single thermocouple for a constant $\Delta T = 3.1$ K. At a constant ΔT, the fiber acts as a constant voltage source, where the maximum current is given by the short circuit current. With an increase in load resistance, the current decreases, but the output voltage increases, and hence there is a maximum in the power output

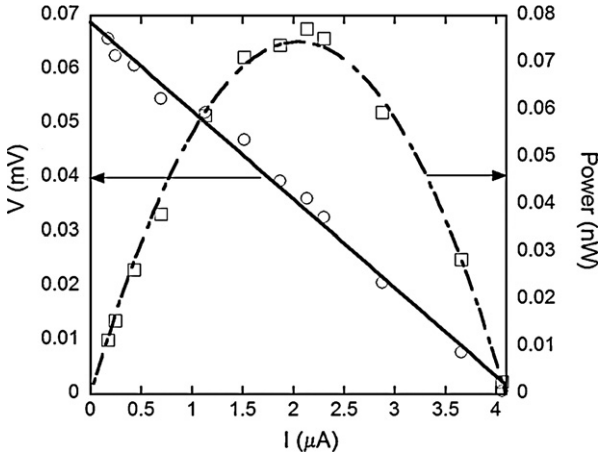

Fig. 3. Power and output voltage as a function of current for $\Delta T = 3.1$ K for 1 couple.

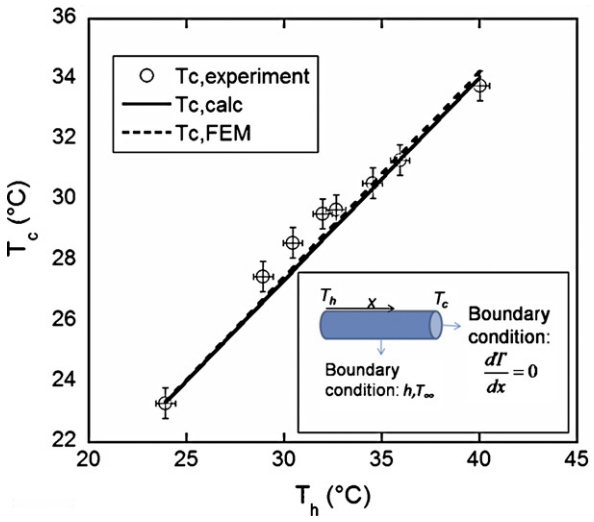

Fig. 4. Temperature of cooler junction as a function of temperature of hotter junction from experiment, fin calculation and FEM simulation. Inset: one dimensional heat transfer along a segment can be modeled as fin heat transfer with adiabatic boundary condition (BC) on end of segment and convection on fiber surface.

at a load resistance that is matched to the resistance of fiber. Increasing the number of thermocouples will increase the maximum output voltage (ΔV_{OC}), as well as the slope of the graph (i.e. fiber resistance, R_f). As Eq. (1) indicates, the power will increase linearly with the number of couples.

In thermoelectric power generators ΔT is often a fixed parameter, given for example by the wall temperature of the heat source and the lowest heat sink temperature accessible via convective cooling. In the case of constant ΔT, the power simply scales as $1/l$ with increasing segment length l, due to an increase in the electrical resistance [14]. Taking into account the effect of contact resistance, an optimization of power can be obtained [15,16]. For fiber-based flexible thermoelectric power generators, one practical configuration would involve a woven thermoelectric fabric wrapped around a hot object, experiencing convective cooling on the opposite side. Under these boundary conditions, both ΔT and resistance can change with segment length, and an optimization in power output can also be obtained. To investigate the optimization conditions for power output, a simple fin heat transfer equation is used to calculate the temperature difference between the hot and cold junctions. The thermal resistances of the thin film and fiber substrate are given by [17]:

$$R_{\text{th,film}} = \frac{l}{\pi(r_2^2 - r_1^2)k_{\text{film}}} \tag{3}$$

$$R_{\text{th,fiber}} = \frac{l}{\pi r_1^2 k_{\text{fiber}}} \tag{4}$$

where r_2 and r_1 are the outer and inner diameters as shown in Fig. 1, k_{fiber} is the thermal conductivity of the fiber, and k_{film} is the thermal conductivity of the thin film. For the silica fiber, the thermal conductivity is 1.2 W mK, and the thermal resistance of both metal films is calculated to be at least 9 times larger than the thermal resistance of the fiber; hence heat transfer through film is neglected. If thicker films of metals were to be used, then the heat transfer through the film would become important. Each segment of fiber can be treated as a fin with a given hot temperature T_h as shown in inset of Fig. 4. Because of the symmetry in the temperature profile, a boundary condition of zero net heat flux ($dT/dx = 0$) is used on both ends of the segment. The temperature in the segment is given by [17]:

$$T(x) = T_\infty + (T_h - T_\infty) \times \frac{\cosh\, m(l-x)}{\cosh\, ml} \tag{5}$$

where T_∞ is the ambient temperature which is assumed to be 22 °C and m is given by [17]:

$$m = \sqrt{\frac{4h}{k_{\text{fiber}} D}} \tag{6}$$

where h is the heat transfer coefficient and D ($= 2r_1$) is the diameter of the fiber. The heat transfer coefficient is obtained by fitting the experimentally obtained T_c with that calculated from Eq. (5). For a value of $h = 7.8$ W m^2 K, a good match between experiments and calculation is obtained. This value is consistent with the cooling of a small surface by natural convection. Fig. 4 shows the T_c obtained from Eq. (5), finite element modeling (FEM) simulations using ANSYS^{TM} [18], and experimental data. Eq. (5) gives a good match with experiments. The FEM simulations where exact modeling is done also show the same T_c, further verifying the model.

Fig. 5 shows the predicted power obtained per couple versus the segment length for Ni–Ag thermocouples with the same film thickness as in the experiments. Using Eq. (5), ΔT can be calculated, and the net power per couple can be written as:

$$P = \frac{\pi S^2 (T_h - T_\infty)^2 t}{8(\rho_e + \rho_p)} \times \frac{D}{l}\left(1 - \frac{1}{\cosh\sqrt{4h/k_{\text{fiber}} D l}}\right)^2 \tag{7}$$

where t is the thickness of films. With an increase in segment length, the resistance of the fiber-based thermoelectric device increases linearly. However, there is also an increase in ΔT, until the maximum ΔT of $T_h - T_\infty$ is obtained. At short segment lengths, the increase in ΔT dominates, and there is an increase in power. At large segment lengths, ΔT saturates at a value of

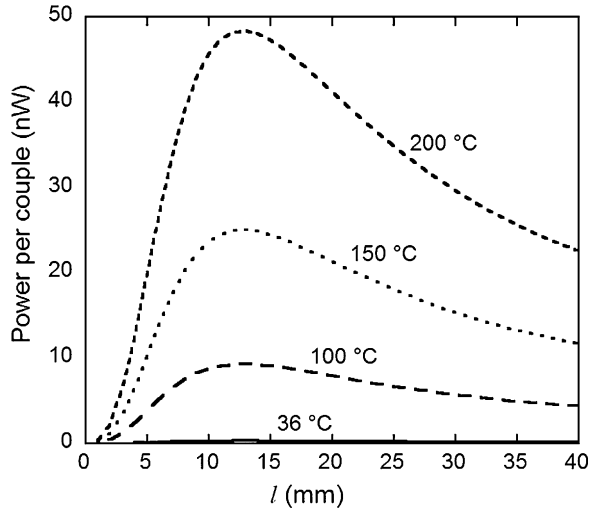

Fig. 5. Power per couple vs. the segment length for different hot junction temperatures.

$T_h - T_\infty$, and the power decreases as $1/l$. A maximum power per couple is obtained by minimizing Eq. (7) with respect to l, yielding an optimization condition for a given diameter of fiber:

$$\sqrt{\frac{4h}{kD}} l_{\max} = 2.44 \tag{8}$$

For the silica fiber having approximately 0.71 mm diameter used in the experiments here, $l_{\max} = 13$ mm is obtained. Smaller diameter fibers would allow a shorter segment length.

Other controllable parameters include the thickness and composition of the deposited thin films. In Fig. 6, the effects of depositing materials with high thermoelectric figure-of-merit (ZT) at different film thicknesses are investigated. The alloy Bi_2Te_3–Sb_2Te_3 is a high ZT material, but for thin films the increase in resistance in using semiconductors can offset the effect of increased thermopower. The Seebeck coefficient for Bi_2Te_3–Sb_2Te_3 is taken to be 375 μV K, and the total resistivity is taken to be 33.5 μ Ω m. These values are adopted from [19], which measured thin films deposited onto glass substrates at 260 °C. Similar values have also been obtained for Bi_2Te_3–Sb_2Te_3 films evaporated on polyimide substrates [20]. For Bi_2Te_3–Sb_2Te_3 thin films having the same thickness as Ni–Ag films, the generated power is predicted to increase by a factor of 5, limited by a comparatively higher resistivity in the semiconductor material. Because semiconductors have lower thermal conductivity than metals, they can be deposited as thicker layers (with correspondingly less electrical resistance) without reducing ΔT due to thermal leakage between the hot side and cold side. Our calculations show that Bi_2Te_3–Sb_2Te_3 films [having thickness] on the order of 2000 nm (still thin enough to remain flexible) can produce an order of magnitude increase in power over 120 nm films.

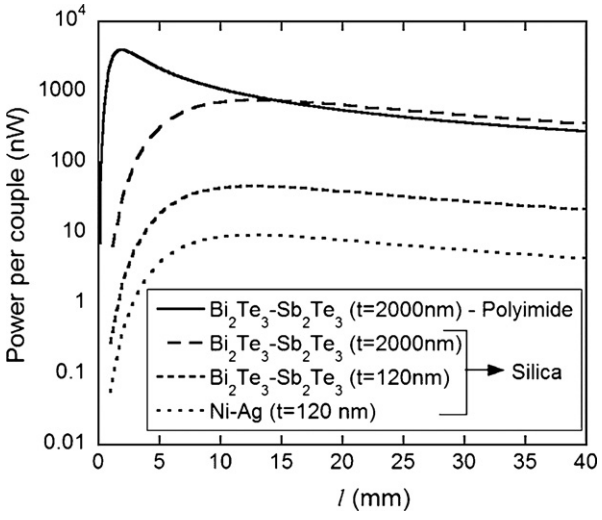

Fig. 6. Comparison of power per couple from Ni–Ag thin films on silica fiber substrate and Bi_2Te_3–Sb_2Te_3 thin films on silica and polyimide fiber substrates for $T_h = 100$ °C.

If polymer fibers such as polyimide are used, rather than silica fibers, an additional advantage of lower substrate thermal conductivity can lead to increased power output. Taking the thermal conductivity of polyimide to be 0.2 W mK [20,21] and the heat transfer coefficient to be the same as that measured for silica fibers, we plot in Fig. 6 the power output per couple for a hollow polyimide fiber of outer diameter 550 μm and inner diameter 500 μm. Convection on the inside of the fiber is neglected, and the ΔT is calculated using Eq. (5). A power output of 1 μW per couple for segment length of 5 mm can be achieved for $T_h = 100$ °C. Hence, hollow polyimide fibers can be good candidates for compact, relatively high power thermoelectric power generators. The lower thermal conductivity of polyimide than that of silica allows a larger $\Delta T/l$ to be maintained, shifting the peak in power generation to shorter segment lengths.

4. Summary

We demonstrated novel fiber-shaped thermoelectric devices comprised of thermally evaporated thin film thermocouples. Open circuit voltage and electrical power output have been measured as a function of temperature difference between the junctions. Using a simple heat transfer analysis, these measurements were extended to different thermocouple segment lengths, material systems and fiber geometries. The combination of our experimental and theoretical analyses in optimizing thermoelectric fiber device performance suggest that this device architecture can be effectively applied in making flexible thermoelectric power generators for waste heat recovery. Utilizing thicker semiconductor films evaporated onto hollow, low thermal conductivity substrates represents an opportunity to further increase power extraction efficiency from heat sources having a variety of shapes.

Acknowledgement

The authors acknowledge the Air Force Office of Scientific research (Contract No. FA9550-06-1-0399) for the financial support of this work.

References

[1] A.I. Casian, in: D.M. Rowe (Ed.), Thermoelectrics Handbook: Macro to Nano, CRC Press, London, 2006 (Chapter 36).
[2] C. Lungenschmied, G. Dennler, H. Neugebauer, S.N. Sariciftci, M. Glatthaar, T. Meyer, A. Meyer, Solar Energy Mater. Solar Cells 91 (2007) 379.
[3] B. O'Connor, K. H. An, Y. Zhao, K. P. Pipe, M. Shtein, Adv. Mater., in press.
[4] J.J. Allen, A.J. Smits, J. Fluids Struct. 15 (2001) 629.
[5] F. Mohammadi, A. Khan, R.B. Cass, MRS Symp. 736 (2002) D5.5.1.
[6] J.A. Paradiso, T. Starner, IEEE Pervasive Comput. 4 (2005) 18.
[7] K. Itoigawa, H. Ueno, M. Shiozaki, T. Toriyama, S. Sugiyama, J. Micromech. Microeng. 15 (2005) S233.
[8] N. Sato, M. Takeda, Proceedings of the International Conference on Thermoelectrics, Clemson University, 24th, 2005, p. 175.
[9] A.P. Ghosh, L.J. Gerenser, C.M. Jarman, J.E. Fornalik, Appl. Phys. Lett. 86 (2005) 223503.
[10] A. Dhawan, T.K. Ghosh, A.M. Seyam, J. Muth, MRS Symp. 736 (2002) D1.9.1.
[11] R. Syukri, Y. Ito, T. Ban, Y. Ohya, Y. Takahashi, Thin Solid Films 422 (2002) 28.
[12] W. Zhang, S.H. Brongersma, O. Richard, B. Brijs, R. Palmans, L. Froyen, K. Maex, Microelectron. Eng. 76 (2004) 146.
[13] F.J. Blatt, P.A. Schroeder, C.L. Foiles, D. Greig, Thermoelectric Power of Metals, Plenum press, New York, 1976, pp. 5 & 149.
[14] S.W. Angrist, Direct Energy Conversion, Allyn and Bacon Inc., Boston, 1982, pp. 121–175.
[15] G. Min, D.M. Rowe, in: D.M. Rowe (Ed.), CRC Handbook of Thermoelectrics, CRC Press, London, 1995 (Chapter 38).
[16] D.M. Rowe, G. Min, J. Power Sources 73 (1998) 193.
[17] F.P. Incropera, D.P. DeWitt, Fundamentals of Heat & Mass Transfer, John Wiley & Sons, New York, 2002, pp. 126–133.
[18] http://www.ansys.com.
[19] L.W. da Silva, M. Kaviany, C. Uher, J. Appl. Phys. 97 (2005) 114903–114911.
[20] L.M. Goncalves, C. Couto, J.H. Correia, P. Alpuim, G. Min, D.M. Rowe, Proceedings of the International Conference on Thermoelectrics, University of Vienna, 26th, 2006, p. 327.
[21] http://www.dupont.com.